

Comparison between backward probability and particle tracking methods for the delineation of well head protection areas

Tiziana Tosco · Rajandrea Sethi

Received: 30 December 2008 / Accepted: 2 June 2009 / Published online: 17 June 2009
© Springer Science+Business Media B.V. 2009

Abstract In this work, a deterministic and a probabilistic method for the delineation of well head protection areas are applied and compared. The deterministic method was implemented using the automatic backward particle tracking algorithm (APA, Tosco et al., *Water Resour Res*, 44(7):W07419, 2008). The backward probability model rests upon the backward adjoint-based model developed by Neupauer and Wilson, and allows the inclusion of dispersion in the definition of capture zones. The two methods are evaluated comparing the “advective front” of the probability protection area and the perimeter given by the particle tracking method. Furthermore, a semi-quantitative study was performed over probability protection areas, in order to evaluate the influence of dispersivity on the extent and growth rate of capture zones identified by fixed probability isolines.

Keywords Capture zones · Backward modelling · Well head protection area (WHPA) · Adjoint equation

1 Introduction

The delineation of Well Head Protection Areas (WHPAs) is usually performed with methods based on the concept of time of travel (TOT): a time is fixed, and the corresponding region of the aquifer is identified, in which the water particles reach the pumping well. For TOT-based WHPAs, both deterministic and probability methods can be used. A deterministic capture area (D-WHPA) is identified by a perimeter, i.e. the boundary line separating the region inside which the water will reach the pumping well within the fixed TOT, and the region in which a higher time of travel would be required to reach the pumping well. On the other hand, the probability methods result in capture areas expressed in terms of probability maps (P-WHPAs).

T. Tosco · R. Sethi (✉)
DITAG – Dipartimento del Territorio, dell’Ambiente e delle Geotecnologie, Politecnico di Torino,
Corso Duca degli Abruzzi 24, 10129, Torino, Italy
e-mail: rajandrea.sethi@polito.it
URL: <http://www2.polito.it/ricerca/groundwater/>

The deterministic methods were developed first. In the past, analytical solutions, such as the Bear and Jacob equation [1], and analytical-graphic methods like the one proposed by Javandel and Tsang [2], and others, were commonly used because of their simplicity. However, they are effective only under very restrictive assumptions. At present, semi-analytical and numerical methods are generally used for WHPA delineation. They can be easily implemented in case of anisotropy, non-homogeneity, and complex geometry [3]. They are also easily coupled with any flow simulation code. In particular, the backward particle tracking model developed by Pollock [4] is the most common methodology. Being a backward method, the particle tracking time-related capture zones can be computed with only one simulation, and the perimeter of the capture area is then delineated by the final positions reached by the particles after a simulation time equal to the fixed TOT. In this way, the backward particle tracking model defines WHPAs in deterministic terms. An Automatic Protection Area (APA) delineation procedure in 2D geometry was recently developed and presented by the authors of this paper [5], and it is here employed for backward particle tracking. Another automatic delineation procedure was proposed by Shafer [6]. However, the delineation of a closed capture area with the particle tracking methodology is much more complicated for a 3D geometry, and complex algorithms are to be implemented. Although less used and more complex, the probability methods allow us to take into account the uncertainty related to our knowledge of the distribution of aquifer parameters. They also make it possible to include this uncertainty into the WHPA delineation, resulting in capture zones expressed as capture probability maps (or capture zone perimeters associated with their confidence limits).

In this work, the deterministic backward particle tracking model is compared to a backward probability model, based on the adjoint of the transport equation which was derived by Neupauer and Wilson [7]. A similar approach was also used by Cornaton and Perrochet, in order to evaluate the groundwater age and travel time in aquifer systems [8,9]. The backward probability model describes the spreading of a capture probability, generated in the pumping well, which moves backwards along the flow direction, according to advection-dispersion phenomena [10–12]. A value of capture probability, similarly to a concentration distribution, is associated to every point of the domain, and a time-related capture probability map can be obtained with only one backward simulation. However, probability capture zones can also be (and must be, in practical applications) reduced to a closed area, by identifying a “limit” probability and the corresponding isoline.

The backward probability model was first developed by Neupauer and Wilson [7] for the identification of the most likely position of a contamination source. Suggestions on how to adapt the backward probability equation to WHPAs are also given by Neupauer and Wilson [10,13]. Frind et al. [11] showed how to manage the modified equation for WHPA delineation using existing transport codes, and in particular for 3D complex geometries. The complete equation characterizing the backward probability transport is here directly derived for the application to capture zones, and subsequently briefly discussed. Furthermore, no quantitative comparison between the backward particle tracking method and the backward probability model has been reported in the literature. For this reason, in the second part of this work, the analysis focuses on the differences, in shape and extent, between the deterministic capture zone and the area included by the 0.5 capture probability isoline, that can be taken as a first approximation of the advective front of the probability plume. A few case studies are presented in order to understand when the two methodologies can be considered equivalent, and when they provide different results. The importance of spatial discretization and the influence of boundary conditions are underlined and a qualitative analysis of the influence of the hydrodynamic dispersion and of the limit probability is presented.

2 Probability model: the backward probability method

Neupauer and Wilson [7] developed the backward probability model working from the advection-dispersion equation (ADE). In particular, if the purpose is the delineation of WHPA, the appropriate equation is the ADE for a conservative solute. The ADE describing the transport in a porous saturated medium of a contaminant neither degraded nor delayed by sorption in a generic domain Ω can be written in the divergence form as:

$$-\vartheta \frac{\partial C}{\partial t} + \frac{\partial}{\partial x_i} \left(\vartheta D_{ij} \frac{\partial C}{\partial x_j} \right) - \frac{\partial(\vartheta v_i C)}{\partial x_i} + q_I C_I - q_O C = 0 \tag{1}$$

$$C(x_i, 0) = C_0(x_i) \quad \text{on } \Omega \tag{1a}$$

$$C(x_i, t) = C_1(x_i, t) \quad \text{on } \Gamma_1 \subset \partial\Omega \tag{1b}$$

$$\left[D_{ij} \frac{\partial C}{\partial x_j} \right] \cdot \vec{n}_i = \overline{q_{n,2}}(x_i, t) \quad \text{on } \Gamma_2 \subset \partial\Omega \tag{1c}$$

$$\left[v_i C - D_{ij} \frac{\partial C}{\partial x_j} \right] \cdot \vec{n}_i = \overline{q_{n,3}}(x_i, t) \quad \text{on } \Gamma_3 \subset \partial\Omega \tag{1d}$$

where $i, j = x, y, z$, D_{ij} is the i,j -th element of the dispersion tensor, ϑ is the porosity, $q_I C_I$ and $q_O C$ represent, respectively, the sources and sinks of contamination, v_i is the effective flow velocity along the x_i direction, C_0 is the initial concentration distribution, Γ_1, Γ_2 and Γ_3 are the portions of the domain boundary $\partial\Omega$ at which the first, second and third type boundary conditions are respectively applied, C_1 is the given concentration at the first type boundaries Γ_1 , n_i is the normal unit vector in the i -th direction, and $\overline{q_{n,2}}$ and $\overline{q_{n,3}}$ are the mass flow rates per unit volume at the second and third type boundaries Γ_2 and Γ_3 , respectively.

Equation 1 is a forward model: the simulation is carried out forwards in space and time to define the contaminant position at a fixed time. The equation can also be easily re-written in terms of forward capture probability: for this purpose the concentration C is substituted by a probability p_t , describing the probability that a solute particle, released at a known contamination source at $t = 0$, would reach a point X of the model domain after a simulation time t^* [13]. The corresponding cumulative distribution function, P_t , can be used in the layout of capture zones (the particle reaches X in a time $t \leq t^*$). The probabilities p_t or P_t are easily calculated using Eq. 1 if the contamination source (the starting point X) is known, but this is not the case of capture zones: it would be necessary to run the transport model for each cell of the domain, and then combining the results. For reasons similar to the particle tracking model, a backward model would be more appropriate. Starting from the ADE and using a variational analysis, Neupauer and Wilson [7, 13] derived the adjoint of the ADE, which is structured as a backward model, i.e. it describes the advective-dispersive transport of a certain variable in the opposite direction of the flow field and backwards in time, in a saturated porous medium. When applied to capture zone delineation, the variable that moves and spreads in the aquifer is the probability P_t : the pumping well is considered a continuous probability source which generates a probability plume (as in forward models, where a source of contamination generates a contaminant plume) [14, 15]. The advective-dispersive backward transport of the probability P_t is modelled by

$$-\vartheta \frac{\partial P_t}{\partial \tau} + \frac{\partial}{\partial x_i} \left(\vartheta D_{ij} \frac{\partial P_t}{\partial x_j} \right) + \frac{\partial}{\partial x_i} (\vartheta v_i P_t) - q_I P_t = -Q(x_i, w) S_w \tag{2}$$

$$P_t(x_i, 0) = 0 \quad \text{on } \Omega \quad (2a)$$

$$P_t(x_i, \tau) = 0 \quad \text{on } \Gamma_1 \subset \partial\Omega \quad (2b)$$

$$\left[v_i P_t + D_{ij} \frac{\partial P_t}{\partial x_j} \right] \cdot \vec{n}_i = 0 \quad \text{on } \Gamma_2 \subset \partial\Omega \quad (2c)$$

$$\left[D_{ij} \frac{\partial P_t}{\partial x_j} \right] \cdot \vec{n}_i = 0 \quad \text{on } \Gamma_3 \subset \partial\Omega \quad (2d)$$

where the flow velocity v of the forward model of Eq. 1 is substituted by $-v$ [11], $\tau = t_{fin} - t$ is the backward time, which runs in the opposite direction of the forward time t (i.e. from the present to the past), and $Q(x_i, w)$ is the pumping rate of the well w . The term on the right side of the equation is the so called load term, which describes the source of probability (for P-WHPAs, the pumping well). In particular, for capture zone delineation, the term is equal to [10]:

$$S_w = \delta(x_1 - x_{1,w})\delta(x_2 - x_{2,w}) \quad \text{in a 2D geometry} \quad (3a)$$

$$S_w = \delta(x_1 - x_{1,w})\delta(x_2 - x_{2,w}) \frac{B_{x_3}(x_{3w,b}, x_{3w,t})}{x_{3w,t} - x_{3w,b}} \quad \text{in a 3D geometry} \quad (3b)$$

where the $\delta(\cdot)$ functions are Dirac delta functions applied in space (in the x_1 and x_2 directions, respectively). The B_{x_3} is a boxcar function, which distributes the capture probability along the x_3 dimension of the pumping well (between the top, $w_{3,t}$, and the bottom, $x_{3,b}$). The load term S_w is related to the probability source (the pumping well) and thus it is not equal to zero only at the pumping well. The term locates a cumulated distribution function of 1 at the pumping well during the entire simulation. Formally, the right side of the equation can be transferred into a first type boundary condition in the backward model. As for the initial and boundary conditions (2a)–(2d), they are slightly different from those of the forward transport model, and are applied, respectively, at the same boundaries Γ_1 , Γ_2 and Γ_3 where the conditions (1a)–(1d) are applied. The second type boundaries of the forward model become third type boundaries in the backward model, and vice versa (see Eqs. 1, 2).

Provided that the chosen parameters are correct and representative, the application of the backward probability model is quite simple. If the flow and transport problems are solved using a code that couples the two equations, a modification of the source code for the transport equation is required. Otherwise, if the two equations are solved separately (eg. with MODFLOW [16] and MT3DMS [17]) the implementation is simplified: it is necessary to reverse the flow field and to modify some boundary conditions of the transport model, which can be directly used to solve the backward transport problem. The following procedure was conducted for this study:

- solution of the forward flow problem using MODFLOW 2000;
- inversion of the flow field using a Matlab script, implemented for this purpose;
- solution of the transport problem with the new boundary conditions and the reversed flow field, using MT3DMS;
- interpretation and post-processing of the results in terms of probabilities.

The appropriate boundary conditions for the implementation of the backward transport problem and for the discretization of the load term are chosen according to Neupauer and Wilson [10]. In particular, the load term is approximated with a first type boundary condition at the well cell. In a 2D geometry, a constant probability of 1 is applied at the well cell, while in a 3D geometry the boxcar function of Eq. 3b is approximated distributing the unit probability along the layers containing the well, making sure that its integral along the vertical direction is equal to 1.

3 Deterministic model: backward particle tracking

In general, when the particle tracking method [4] is applied, a circle of equally spaced particles is located around the pumping well and traced backwards. The capture zone encirclement at the desired travel time is then performed manually, connecting the end points reached by the particles at the fixed time. Consequently, equally spaced particles can be inefficient in case of strong heterogeneities in the aquifer parameters distribution, thus requiring a very high number of particles. In addition, if a limited number of traces is employed, the perimeter can be inaccurately defined near the stagnation points. The APA algorithm presented in [5] overcomes these problems. This algorithm involves a hybrid forward-backward two-step procedure, based on a numerical calculation of the stagnation point of each well, and further refinements. Forward and backward particle tracking algorithms are coupled, and a post-processing algorithm interpolates the pathlines and delineates closed capture zone perimeters for fixed TOTs in a completely automatic way. The algorithm is structured in three steps:

- APA-I: the position of the stagnation point of each well is identified, and the initial position and radius of two circles of particles is defined;
- APA-II: two particle tracking simulations are performed. For each well, a circle of equally spaced particles around the pumping well is traced backwards, while a circle of particles around the stagnation point is traced forwards. The resulting pathlines are processed and new starting positions for backward (not equally spaced) particles around the pumping well are defined;
- APA-III: the results of a second (fully) backward simulation are elaborated by a post-processing interpolation algorithm.

4 Comparison between D-WHPAs and P-WHPAs

As previously explained, for practical applications of a probability method in the delineation of WHPAs, a limit probability (or more than one) has to be adopted to identify the capture zone as a closed area: probability capture zone perimeters also have to be defined identifying a “limit” probability and the corresponding isoline. The extent of a D-WHPA depends on the value of the aquifer parameters and on the travel time, while the extent of a P-WHPA also strongly depends on the limit probability, which results from the desired level of protection. It is therefore to be determined by the decision maker, rather than by the modeler.

If compared to the particle tracking approach, the P-WHPAs are characterized by a dependence on hydrodynamic dispersion and on probability levels. It follows that the higher the dispersivity value, the higher will be the uncertainty in the aquifer characterization, and the larger will be the capture area, for fixed travel times and capture probabilities. Based on these considerations, the influence of the mentioned parameters (travel time, dispersivity and capture probability) on the extent of the capture area is here investigated.

For a given dispersivity value α , the capture area A identified by the isoline corresponding to a probability level P for a travel time TOT, can be written as the sum of two contributions, an “advective” and a “dispersive” one:

$$A(P, TOT; \alpha) = A_{Adv}(TOT) + A_{Disp}(P, TOT; \alpha) \tag{4}$$

The advective contribution is always positive, it is equal to the area of the D-WHPA and it depends on the travel time. For a homogeneous, isotropic aquifer with a constant thickness and a fully-penetrating well, it depends on the pumping rate Q , the aquifer thickness b , the effective porosity n_e and the time t according to the following expression:

$$A_{Adv}(t) = \frac{Q}{bn_e} t \quad (5)$$

where $Qt = Abn_e$ is the volume of water extracted during a time t .

The dispersive contribution, on the contrary, depends on all three mentioned parameters, and can be either positive or negative.

The effects of the variation of capture probability and dispersivity on the extent of P-WHPAs can be easily investigated if the “growing rate” of the capture area is considered, rather than the area itself:

$$\frac{dA}{dt} = \frac{dA_{Adv}}{dt} + \frac{dA_{Disp}}{dt} \quad (6)$$

The advective contribution can be directly obtained by differentiating Eq. 5. The dispersive contribution can be similarly modelled, leading to the following expression:

$$\frac{dA}{dt} = \frac{dA_{Adv}}{dt} + \frac{dA_{Disp}}{dt} = \frac{Q}{bn_e} (1 + C_{Disp}) \quad (7)$$

and therefore:

$$\frac{\frac{dA_{Disp}}{dt}}{\frac{dA_{Adv}}{dt}} = C_{Disp}(TOT, P; \alpha) \quad (8)$$

where C_{Disp} represents the growth rate of the dispersive contribution normalized to the advective one, and depends on the geometry of the problem, the parameter values (in particular, the dispersivity), the capture probability and the travel time. Also in this case, the dispersive contribution is negative for capture probabilities $P > 0.5$, as will be shown in the applications below. A high absolute value of C_{Disp} then means that the dispersion phenomenon is acting on the shape and extent of the capture area, and thus its effects could be taken into account when defining WHPAs. In the following paragraphs, D-WHPAs and P-WHPAs calculated for three case studies are presented and compared, using the relation of Eq. 7.

5 Applications

The particle tracking and the backward probability models were applied to the three case studies presented in [5], i.e. three confined 2D aquifers. The dispersive contribution to the extent of the capture areas was determined using Eq. 7. The three test cases are:

- *case 1*: one pumping well in a confined, homogeneous, isotropic aquifer, with the main flow direction along the y axis, hydraulic conductivity $K = 7.5 \times 10^{-5}$ m/s.
- *case 2*: four pumping wells in a confined, homogeneous, isotropic aquifer with the main flow direction along the y axis, hydraulic conductivity $K = 7.5 \times 10^{-5}$ m/s;
- *case 3*: one pumping well in a confined, heterogeneous, isotropic aquifer, with the main flow direction oriented along the diagonal of the domain, hydraulic conductivities $K_1 = 2.0 \times 10^{-4}$ m/s and $K_2 = 5.0 \times 10^{-5}$ m/s. The conductivities are constant within square sub-domains of $1,200 \text{ m} \times 1,200 \text{ m}$ (Fig. 3a).

In all cases, the aquifer was represented by one layer, 10 m thick, and divided into square $25 \text{ m} \times 25 \text{ m}$ cells. The model domain used in [5], designed as a $3,600 \text{ m} \times 3,600 \text{ m}$ square domain (origin of the axes in the lower left corner), is here extended to evaluate the behaviour of the probability capture areas over long travel times (up to over 20 years). The domain for cases 1 and 2 was then extended 700 m east and west, and 6,400 m north, reaching the dimensions of

5,000 m along the x axis and 10,000 m along the y axis. For case 3, the domain was extended 3,600 m west and 3,600 m north. In case 1 and 2, the main flow direction is in the negative y direction, from north to south. The applied flow boundary conditions are two Dirichlet conditions, at the north and south boundaries, resulting in a regional gradient equal to 1.67×10^{-2} . The left and the right boundaries are no flow boundaries. In case 3, four Dirichlet conditions are applied, and a linearly-changing-in-space and constant-in-time head is applied along them, resulting in a mean flow direction along the diagonal of the cells. In case 1 and 3, the pumping well is located at $x = 1,812.5 \text{ m}, y = 1,437.5 \text{ m}$, with a pumping rate of $2.0 \times 10^{-2} \text{ m}^3/\text{s}$. In case 2, the four pumping wells extract $2.5 \times 10^{-2} \text{ m}^3/\text{s}$ altogether ($Q = 5.0 \times 10^{-3} \text{ m}^3/\text{s}$ for pumping wells W_1, W_2, W_3 ; $Q = 1.0 \times 10^{-2} \text{ m}^3/\text{s}$ for W_4). The pumping well W_1 is located at $x = 1,812.5 \text{ m}, y = 1,437.5 \text{ m}$; W_2 at $x = 1,412.5 \text{ m}, y = 1,437.5 \text{ m}$; W_3 in $x = 2,212.5 \text{ m}, y = 1,437.5 \text{ m}$; W_4 at $x = 1,812.5 \text{ m}, y = 1,037.5 \text{ m}$ Values of longitudinal dispersivity ranging from 5 to 125 m were considered. The transverse dispersivity was set equal to 1/10 of the longitudinal dispersivity.

The steady state flow field was solved with MODFLOW 2000 using the WHS solver [16], the backward particle tracking using the APA algorithm on MODPATH [4] simulations, the backward probability model with a Matlab script for the inversion of the flow field and MT3DMS [17] for the transport problem, using the third-order Total Variation Diminishing (TVD) method. A fictitious conservative contaminant, which represents the backward probability, was employed. The load term of Eq. 3 was discretized using a first type boundary condition of constant capture probability: a capture probability of 1 was used at the pumping well during the transport simulation. A second type boundary condition of zero probability gradient was applied at all the external boundaries of the model domain (the condition is automatically obtained by the cell-centred finite difference models, as explained above).

The capture areas for several travel times were determined using both the particle tracking and the backward probability method. The isoline for $P = 0.5$ in the capture probability plume has been compared with the deterministic perimeter given by the particle tracking simulation.

5.1 Comparison between D-WHPAs and P-WHPAs

The results for the three test cases are reported in Figs. 1, 2, 3 and 4. Initially, a longitudinal dispersivity of 50 m was considered. The differences in shape and extent between the D-WHPA and the P-WHPA for a capture probability of 0.5 were analyzed. First, for each case study, a comparison of the shape of the areas obtained with the three methods is reported (Figs. 1, 2, 3). Secondly, a more quantitative comparison is presented: a normalized difference ΔA between the extent of the deterministic area A_{Adv} (see Eq. 5) and the surface area included in the 0.5 capture probability isoline $A_{P=0.5}$ was considered (Fig. 4):

$$\Delta A = \frac{A_{Adv} - A_{P=0.5}}{A_{Adv}} \tag{9}$$

In case 1 (one pumping well, homogeneous aquifer) there is no significant difference in shape between the D-WHPA and the area included by the 0.5 probability isoline of the P-WHPA (see Fig. 1). The differences in extent are always <10% (Fig. 4a). They are more evident at low travel times, when the influence of the transport boundary condition at the pumping well and the effects of the spatial discretization (irregular shape of the curves) play an important role. Furthermore, they slightly increase at very long travel times, when the capture probability plume approaches the boundaries of the model domain. In this case, the second type homogeneous boundary conditions, used as an approximation for boundary conditions (2c),

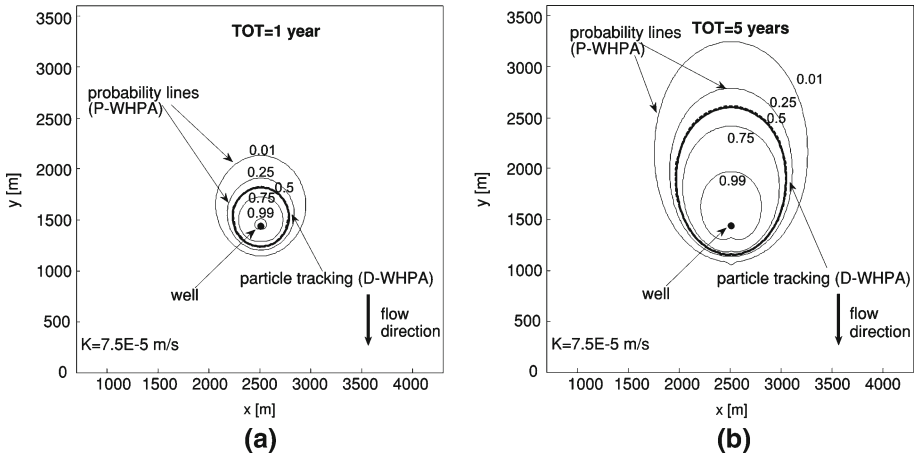


Fig. 1 Case 1: comparison between backward probability capture area (P-WHPA) and particle tracking capture area (D-WHPA). P-WHPAs are plotted for several capture probabilities and their shape is compared to the D-WHPA perimeter, at TOT = 1 year (a), and TOT = 5 year (b). A good agreement between the D-WHPA (dashed line) and the 0.5 isoline of the P-WHPA (thicker continuous line) can be observed

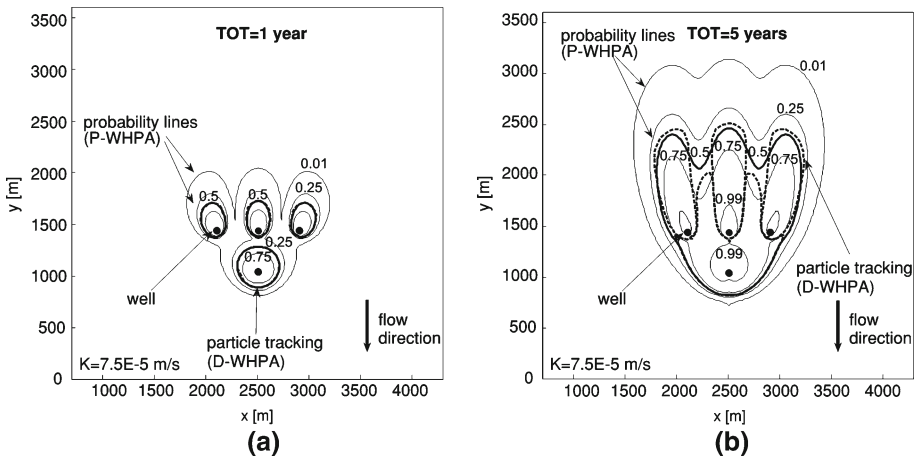


Fig. 2 Case 2: comparison between backward probability capture area (P-WHPA, 0.5 isoline as a thicker continuous line) and particle tracking capture area (D-WHPA, dashed line). P-WHPAs are plotted for several capture probabilities and their shape is compared to the D-WHPA perimeter, at TOT = 1 year (a), and TOT = 5 year (b). For TOT = 5 years, big discrepancies are evident, both in shape and extent

as suggested by Neupauer and Wilson [10] and Frind et al. [11], are no longer accurate, as the probability plume approaches the exit of the model domain, and the results are thus influenced. More in general, discrepancies with respect to the theoretical advective contribution increase as the dispersivity increases, i.e. when the capture probability plume is more dispersed and approaches the domain boundaries earlier. However, at intermediate travel times, at which the capture zones are usually calculated (between 180 days and 5 years), ΔA is closer to zero, not being strongly affected by boundary conditions at the pumping well or at the borders of the domain, nor by the load term definition.

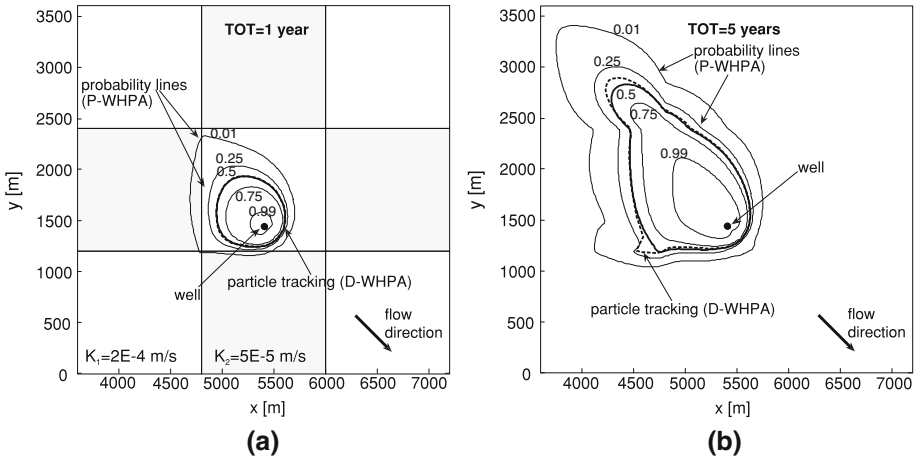


Fig. 3 Case 3: comparison between backward probability capture area (P-WHPA, 0.5 isoline as a thicker continuous line) and particle tracking capture area (D-WHPA, dashed line). P-WHPAs are plotted for several capture probabilities and their shape is compared to the D-WHPA perimeter, for TOT = 1 year (a), and TOT = 5 year (b). The spatial distribution of conductivity is also reported (a). For a TOT of 5 years, the P-WHPA is shown to be more smoothed, the D-WHPA being more affected by abrupt changes in conductivity

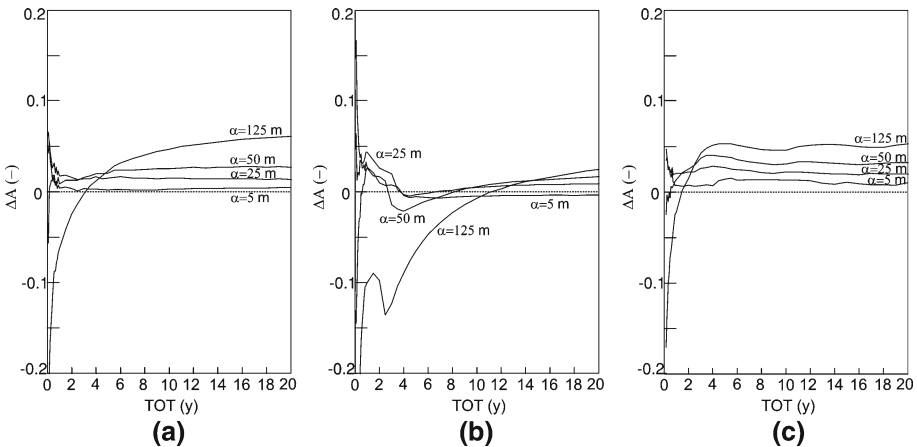


Fig. 4 Normalized differences ΔA are plotted for the 0.5 probability isoline of P-WHPAs for cases 1 (a), 2 (b) and 3 (c). The graphs highlight the influence of boundary conditions on the accuracy of the P-WHPA. For multiple pumping wells (b), the importance of dispersion in the P-WHPAs delineation is shown by the negative peaks of the curves, corresponding to the merging of probability plumes for different pumping wells. Dashed lines at $\Delta A=0$ are reported to guide the eye

For case 2, differences in both shape and extent between the D-WHPA and the 0.5 probability isoline are more evident at intermediate travel times (Fig. 2). The differences in shape increase with the travel time as represented in Fig. 2b. For short times, the four P-WHPAs are completely or partially separated, and differences with respect to the D-WHPAs are not evident. For longer times, however, the 0.5 isolines of the single wells approach each other and merge, thus leading to an overall area larger than the one estimated by the D-WHPAs, and also different in shape. This corresponds to negative values of ΔA (Fig. 4b), observed at

travel times of a few years. Furthermore, the differences increase as the dispersivity increases, being generated by a physical phenomenon (dispersion), rather than numerical approximations (influence of the spatial discretization and the boundary conditions), as for cases 1 and 2. In the region between two different pumping wells, the transverse dispersive contribution to the transport of the capture probability of each well generates non-negligible values, which are summed in the overall P-WHPA. This region cannot be included in any way into the deterministic perimeter, thus it is neglected.

In case 3 (one pumping well, heterogeneous aquifer), for short travel times (Fig. 3a) there is a quite good agreement between the 0.5 probability isoline and the advective area. However, as the simulation time increases, shape differences become more evident: the deterministic capture zone extends more along and perpendicularly to the flow direction, as it enters new regions with a higher conductivity value (Fig. 3b). This means that particles move faster than the capture probability plume when they leave zones at lower conductivity and enter zones at higher conductivity. The final result is a more smoothed shape for the probability capture zone in case of abrupt heterogeneous in the aquifer, compared to the deterministic one, as already outlined by Frind et al. [11, 12]. However, the normalized difference between the deterministic capture area and the 0.5 probability isoline (Fig. 4c) is always relatively small (<5% even at very long travel times). This means that, although the shape of the capture zone is quite different, its extent is not.

5.2 P-WHPAs: role of dispersivity and capture probability

Capture areas were then calculated for travel times up to about 20 years, over the extended model domain, to investigate the long-term influence of hydrodynamic dispersion and of the chosen limit probability on completely developed capture areas. The simulations were stopped when the 0.01 probability isoline approached the domain boundaries. Simulations were run for various dispersivities, as mentioned previously, and capture probability isolines were calculated for probabilities ranging from 0.01 to 0.99.

In Figs. 5, 6 and 7 the coefficient C_{Disp} of Eq. 8 is reported as a function of the travel time. C_{Disp} defines the importance of the advective growth rate of the capture area with respect of the theoretical value of the advective growth rate, Q/bn_e . Negative values are related to negative dispersive growth rates, positive values to positive growth rates, the advective contribution always being positive. Plots for case 1 (Fig. 5) are smoothed and more regular than the others, but a common trend can be identified in all three cases. The capture areas identified by the isolines for probabilities higher than 0.5 are characterized by negative coefficients, resulting in a total rate dA/dt lower than the constant advective contribution Q/bn_e , for any travel time and dispersivity employed (see Figs. 5, 6 and 7). Furthermore, for any fixed value of capture probability, the higher the dispersivity, the lower is C_{Disp} .

The opposite holds for probabilities lower than 0.5: C_{Disp} is positive, i.e. the growth rates are always higher than Q/bn_e , and increase as the dispersivity increases. This means that, for short travel times, the isolines are close one to each other (as evident in Figs. 1, 2 and 3), and become more and more distant as the travel time increases. The behaviour is more evident at high dispersivities. In all cases, for long travel times (corresponding to completely developed capture zones), the increase/decrease of the growth rate dA_{Disp}/dt is clearly constant.

For simple cases, with one pumping well and homogeneous parameter distributions (case 1), oscillations of C_{Disp} in time are not very significant, and lose importance for long-term WHPAs, when the capture zone is completely developed (Fig. 5). This general trend, however, is partially altered in cases 2 and 3. For multiple wells (case 2, Fig. 6), important, systematic variations in the general trend happen at low-intermediate travel times, for every

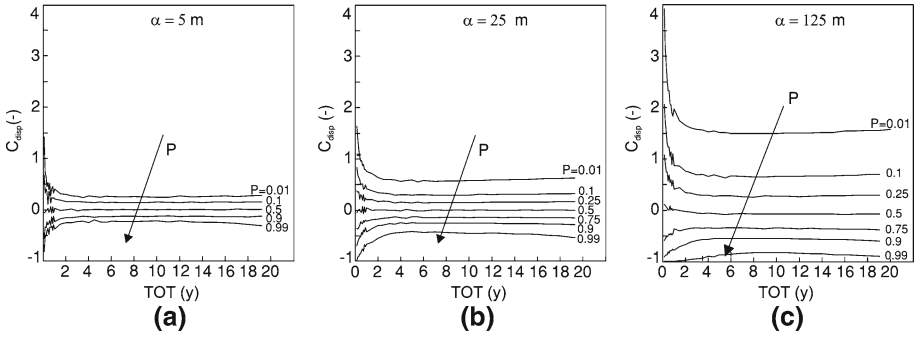


Fig. 5 Case 1: plots of the coefficient C_{Disp} in Eq. 8, representing the relative importance of the dispersive contribution to the capture area, with respect to the advective one. C_{Disp} is reported as a function of time, for small (a), medium (b), and large (c) dispersivities, and for different capture probabilities

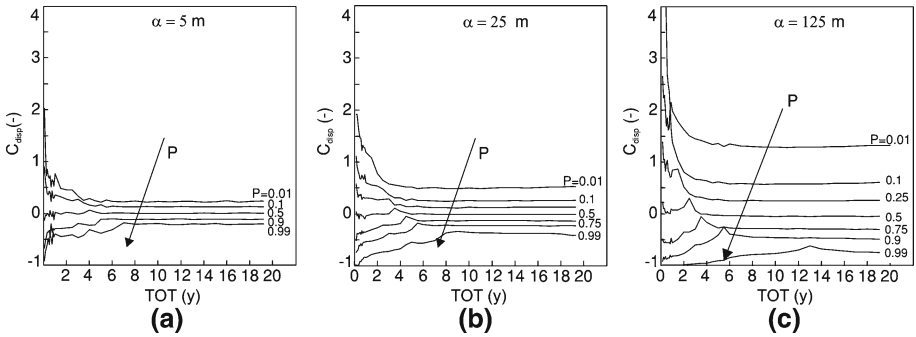


Fig. 6 Case 2: plots of the coefficient C_{Disp} in Eq. 8, representing the relative importance of the dispersive contribution to the capture area, with respect to the advective one. C_{Disp} is reported as a function of time, small (a), medium (b), and large (c) dispersivities, and for different capture probabilities. Peaks at small-medium travel times correspond to the merging of the probability plumes of the pumping wells

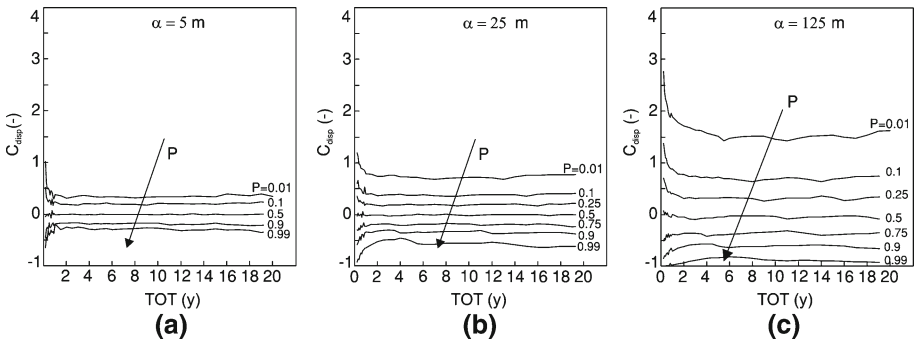


Fig. 7 Case 3: plots of the coefficient C_{Disp} in Eq. 8, representing the relative importance of the dispersive contribution to the capture area, with respect to the advective one. C_{Disp} is reported as a function of time, for small (a), medium (b), and large (c) dispersivities, and for different capture probabilities. Oscillations at long travel times reflect the inclusion in the capture zone of squared sub-domains with different conductivities

capture probability, and are mainly due to the merging of the capture zones of different wells, thus deriving from a real physical phenomenon, rather than numerical approximations. For every fixed capture probability, the main peak corresponds to the moment at which the isolines of the four probability plumes merge (see for comparison Fig. 4b). This time is of course smaller for small capture probabilities (corresponding to larger areas), if the dispersivity is fixed, and smaller for larger dispersivities, if the capture probability is fixed. In addition, a secondary peak at lower times can also be identified, which corresponds to the merging of the probability isoline of the two central wells. In case 3, on the contrary, the fluctuations are also present at long travel times, and reflect the heterogeneities in the conductivity distribution (one oscillation for every square sub-domain with high conductivity, see Figs. 3b, 7). It can also be noticed that such oscillations are more evident for high dispersivities: in this case the probability plume involves larger areas, and consequently a higher number of sub-domains with different conductivities.

6 Discussion and conclusions

The application of the backward probability model of Neupauer and Wilson [7] to capture zone delineation allows us to take into account dispersion without high computational costs. The backward probability model includes dispersion into WHPA delineation, and gives capture zones with only one backward simulation, which has the same time cost as an advective-dispersive transport simulation. However, if the model is to be applied to real systems, a good estimate of the dispersion coefficient will be necessary.

The implementation of this model is quite easy, because it can be done with any common transport simulation code, accordingly modified. However, numerical dispersion is to be carefully considered, and future perspectives can take into consideration the use of transport simulators less affected by numerical dispersion than those based on finite difference schemes. Since capture probability is calculated over the entire model domain, the boundaries of P-WHPAs for fixed probabilities can be automatically defined using any simple interpolation over the probability distribution, to obtain an implicit isoline (2D geometry) or iso-surface (3D geometry). On the contrary, the particle tracking methodology always requires post-processing interventions, for a manual or automatic delineation of the areas (eg. the APA algorithm presented in [5]), and the automatic definition of 3D limits involves quite complicated algorithms.

The introduction of a probability component in the model would allow us to fix the perimeter of the protection area in correspondence to a “limit probability”, according to the importance of the water resource, the dangerous centres near it and, more generally, the land management and use. It would be important to establish rules for the determination of this optimal capture probability: if a very low value is selected, the water resource will be more protected, but this could lead to excessive land use limitation. On the contrary, if a high value is adopted, higher than 0.5, the resulting capture zone is even smaller than the corresponding D-WHPA, which can lead to an absolutely inadequate protection of the water resource. However, the application of a probability model for WHPA delineation can be justified in case of multiple wells, also when the 0.5 probability isoline is taken as a limit probability. Public regulations require WHPAs to be delineated at relatively small travel times (180 days, 1 or 5 years), and in this case the differences, both in shape and in extent, between the D-WHPA and the 0.5 isoline of the P-WHPA can be apparent (see case 2 for $TOT = 5$ years, Figs. 2, 4b), and are due to the physics of the phenomenon (the dispersive component of the probability transport). Moreover, the backward probability model can also be successfully applied in case

of heterogeneities in the aquifer parameter distributions, even if the 0.5 capture probability is chosen as the limit probability. In this case, the method results in more smoothed and regular capture areas, if compared to the particle tracking results. Furthermore, the change in shape does not necessarily correspond to a change in the extent of the capture area, but can result in more efficiently defined WHPAs. As a future perspective, an extension of both methods in transient flow conditions can also be considered, which have been previously shown to have a relevant influence on WHPA delineation [18].

The test cases presented above, although simple 2D applications, show the importance of the choice of the spatial discretization and the extent of the model domain. The roughness of the discretization influences the accuracy of the results at low travel times (see the irregular shape of the first part of the curves in Figs. 5, 6 and 7), when the effect of the boundary condition at the pumping well is not negligible. On the other hand, the extent of the model domain influences the behaviour at long travel times, when the approximation of second-type, homogeneous boundaries is incorrect. Plots of the differences between the extent of the theoretical advective capture area (Q/bn_e) and the corresponding area included by the 0.5 probability isoline, like those reported in Fig. 4, highlight the existence of a region at medium travel times, where the influence of the boundary condition is minimal. Such plots could therefore be used in applications of the backward probability model, in order to check the goodness of the choice of the spatial discretization and the extent of the model domain.

References

1. Bear J, Jacobs M (1965) On the movement of water bodies injected into aquifers. *J Hydrol (Amst)* 3(1):37–57. doi:[10.1016/0022-1694\(65\)90065-X](https://doi.org/10.1016/0022-1694(65)90065-X)
2. Javandel I, Tsang CF (1986) Capture-zones type curves: a tool for aquifer cleanup. *Ground Water* 24(5):616–625. doi:[10.1111/j.1745-6584.1986.tb03710.x](https://doi.org/10.1111/j.1745-6584.1986.tb03710.x)
3. Fienen MN, Luo J, Kitanidis PK (2005) Semi-analytical homogeneous anisotropic capture zone delineation. *J Hydrol (Amst)* 312(1–4):39–50. doi:[10.1016/j.jhydrol.2005.02.008](https://doi.org/10.1016/j.jhydrol.2005.02.008)
4. Pollock D (1989) Documentation of computer programs to compute and display pathlines using results from the US geological survey modular three-dimensional finite-difference ground-water model. In: US geological survey, open file report 89-381, Reston, Virginia
5. Tosco T, Sethi R, Di Molfetta A (2008) An automatic, stagnation point based algorithm for the delineation of wellhead protection areas. *Water Resour Res* 44(7):W07419. doi:[10.1029/2007WR006508](https://doi.org/10.1029/2007WR006508)
6. Shafer JM (1987) Reverse pathline calculation of time-related capture zones in nonuniform flow. *Ground Water* 25(3):283–289. doi:[10.1111/j.1745-6584.1987.tb02132.x](https://doi.org/10.1111/j.1745-6584.1987.tb02132.x)
7. Neupauer RM, Wilson JL (1999) Adjoint method for obtaining backward-in-time location and travel time probabilities of a conservative groundwater contaminant. *Water Resour Res* 35(11):3389–3398. doi:[10.1029/1999WR900190](https://doi.org/10.1029/1999WR900190)
8. Cornaton F, Perrochet P (2006) Groundwater age, life expectancy and transit time distributions in advective-dispersive systems: 1. Generalized reservoir theory. *Adv Water Resour* 29(9):1267–1291. doi:[10.1016/j.advwatres.2005.10.009](https://doi.org/10.1016/j.advwatres.2005.10.009)
9. Cornaton F, Perrochet P (2006) Groundwater age, life expectancy and transit time distributions in advective-dispersive systems: 2. Reservoir theory for sub-drainage basins. *Adv Water Resour* 29(9):1292–1305. doi:[10.1016/j.advwatres.2005.10.010](https://doi.org/10.1016/j.advwatres.2005.10.010)
10. Neupauer RM, Wilson JL (2004) Numerical implementation of a backward probabilistic model of ground water contamination. *Ground Water* 42(2):175–189. doi:[10.1111/j.1745-6584.2004.tb02666.x](https://doi.org/10.1111/j.1745-6584.2004.tb02666.x)
11. Frind EO, Muhammad DS, Molson JW (2002) Delineation of three-dimensional well capture zones for complex multi-aquifer systems. *Ground Water* 40(6):586–598. doi:[10.1111/j.1745-6584.2002.tb02545.x](https://doi.org/10.1111/j.1745-6584.2002.tb02545.x)
12. Frind EO, Molson JW, Rudolph DL (2006) Well vulnerability: a quantitative approach for source water protection. *Ground Water* 44(5):732–742
13. Neupauer RM, Wilson JL (2001) Adjoint-derived location and travel time probabilities for a multidimensional groundwater system. *Water Resour Res* 37(6):1657–1668. doi:[10.1029/2000WR900388](https://doi.org/10.1029/2000WR900388)

14. Tosco T, Sethi R, Di Molfetta A (2007) A backward probabilistic model to calculate well head protection areas. In: Candela et al (eds) *Water pollution in natural porous media at different scales. Assessment of fate impact and indicators*. WAPO2 (pp 731–737). Instituto Geologico y Minero de Espana, Barcelona, Spain
15. Tosco T, Sethi R, Di Molfetta A (2006) A probabilistic method for delineation of wellhead protection areas. In: *Fifteenth international symposium on mine planning and equipment selection, MPES, Torino (Italy)*, 20–22 Sept 2006
16. Harbaugh AW, Banta ER, Hill MC, McDonald MG (2000) MODFLOW-2000, the US geological survey modular groundwater model—user guide to modularization concepts and the groundwater process. In: *US geological survey, open file report 00-92*, Reston, Virginia
17. Zheng C, Wang PP (1999) MT3DMS: a modular three-dimensional multispecies transport model for simulation of advection, dispersion, and chemical reactions of contaminants in groundwater systems; documentation and user's guide. *US army engineer research and development center, Vicksburg*
18. Vesselinov VV, Robinson BA (2006) Delineation of capture zones in transient groundwater flow systems. In: Bierkens M et al (eds) *ModelCARE 2005 calibration and reliability in groundwater modeling: from uncertainty to decision making (Proceedings of ModelCARE 2005, The Hague, The Netherlands, June 2005)*. IAHS publication 304, Wallingford, UK, pp 246–252